Enhanced carrier mobilities in two-dimensional electron gases at III-III/I-V oxide heterostructure interfaces

Valentino R. Cooper

Phys. Rev. B **85**, 235109 — Published 5 June 2012

DOI: 10.1103/PhysRevB.85.235109

Enhanced two dimensional electron gases at III-III/I-V oxide heterointerfaces

Valentino R. Cooper*
Materials Science and Technology Division, Oak Ridge National Laboratory, Oak Ridge, TN 37831-6056

Density functional theory is used to explore the electronic reconstruction at III-III/I-V heterointerfaces. It is demonstrated that due to large B-cation valence differences a δ-doped, two dimensional electron gas (2DEG) can be created with an increased intrinsic carrier limit; resulting in interfacial charge densities twice that of prototypical $LaTiO_3/SrTiO_3$. Observed decreases in band effective masses suggest enhancements in carrier mobilities. Unprecedented agreement with recent experiments highlight the fact that it is the electronic structure of the bulk component material that defines the properties of oxide 2DEGs. These geometries provide a more tunable platform through which the underlying physics of electron confinement can be thoroughly examined and thus have implications for modern device applications.

PACS numbers: 73.40.-c, 71.28.+d, 31.15.E-, 81.05.Zx

Emergent phenomena at ABO_3 oxide interfaces, e.g. two dimensional electron gases (2DEGs) [1], are paramount to understanding critical behavior arising from electron confinement; like metal-insulator transitions [2], novel magnetic effects [3] and superconductivity [4, 5]. Exploiting these features may be useful in a range of modern technological applications such as semiconductor [6] and thermoelectric devices [7]. Furthermore, it has been suggested that the incorporation of heavy, 5d, transition metal elements may result in a significant Rashba spin splitting due to enhanced spin-orbit coupling; a key factor for spintronics [8, 9]. Hence, controlling both the mobility and the density of electrons at an interface is crucial for fine tuning these materials for specific device applications as well as providing a foundation for a better understanding of phenomena arising from electron confinement.

A chemically intuitive mechanism, the so-called δ-doped mechanism, presents a rich tapestry through which the electronic structure at an interface can be modulated. Here, 2DEGs are a consequence of the presence of multivalent transition metal cations, like Ti, at a heterointerface comprised of A-site cations with different valence states. For example, in $LaTiO_3/SrTiO_3$ superlattices, the local environment of Ti cations next to a "dopant", LaO layer, splits the valence of Ti between two possible charge states (+4 for $SrTiO_3$ and +3 for $LaTiO_3$). Therefore, an equal mixture of Ti valence states (3+ or 4+) can be thought to reside at the interface giving an average valence of 3.5 [10–12]. This has been confirmed through electron energy-loss spectroscopy (EELS) measurements [13] in which the distribution of Ti^{3+} cations away from the interface were in good agreement with theoretical and experimental carrier density profiles [14–19]. In an ideal system, the extra 1/2 electron, relative to Ti in $SrTiO_3$, defines the intrinsic limit of 2DEG carrier densities [20]. This electronic reconstruction is a hallmark of the observed two-dimensional conductivity and is accompanied by polar distortions [15, 21, 22] (atomic displacements of the cations away from the interface) which effectively screen the electrons near the interfaces. Despite this simple mechanism, to date, most commonly studied 2DEGs involve II-IV (primarily $Sr^{2+}Ti^{4+}O_3$) oxides, where the interfacial carrier densities are intrinsically limited to 0.5 e^-/interface unit cell. Similarly, even fewer efforts have explored 2DEGs in 4d and 5d transition metals.

In this paper, density functional theory (DFT) calculations are used to investigate the charge rearrangement at interfaces between I-V/III-III perovskites. The guiding principle is that the incorporation of a multivalent cation at an interface, where its desired valence states are +3 and +5, should allow for an average valence of +4, thus increasing the limit of extra interfacial charge to 1 e^-/interface unit cell. Here, unlike $LaAlO_3$ and $LaGaO_3$ based heterostructures that require multiple layers to create 2DEGs via the the polar catastrophe mechanism [14, 23–28], it is demonstrated that it is indeed possible to induce a 2DEG in 4d and 5d superlattices comprised of 1 layer of LaXO$_3$ and 7 layers of KXO$_3$, where X=Ta and Nb without oxygen vacancies [14, 29]. More importantly, these heterostructures have a total of 1 electron per interface unit cell now populating the conduction bands (twice that of a corresponding $LaTiO_3/SrTiO_3$ superlattice). Similar to previous observations, these electrons are primarily confined to t_{2g} orbitals on B cations near LaO interfaces, decay quickly into the bulk and are accompanied by large polar ionic distortions. In addition, calculated decreases in electron band effective masses suggest that improved carrier mobilities may be achievable. Remarkable agreement with recent ARPES measurements of surface 2DEGs band effective masses [9, 30] stresses the point that it is the component material's electronic structure that defines the interfacial carrier mobilities in oxide 2DEGs.

DFT calculations using the local density approximation with a Hubbard U (LDA+U) [31] and ultrasoft pseudopotentials [32] as implemented in the Quantum Espresso simulation package [33, 34] were performed to study 1 LaXO$_3$/7 KXO$_3$ superlattices, where X=Ta and

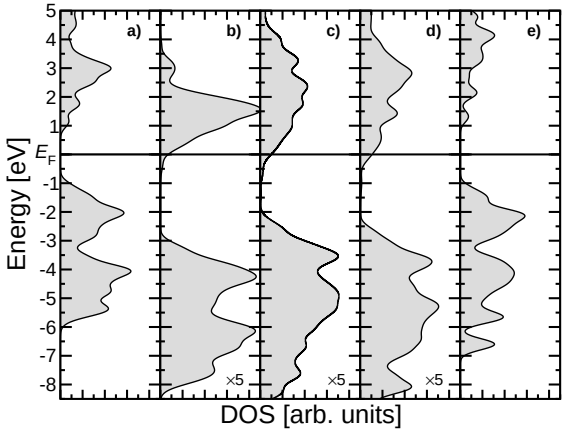

FIG. 1. DOS for (a) bulk $SrTiO_3$, (b) 1 $LaTiO_3$/7 $SrTiO_3$, (c) 1 $LaNbO_3$/7 $KNbO_3$ (d) 1 $LaTaO_3$/7 $KTaO_3$ and (e) bulk $KTaO_3$. All energies are relative to the Fermi level, E_F. (The scale for the heterostructures is 5× that of the bulk structures.)

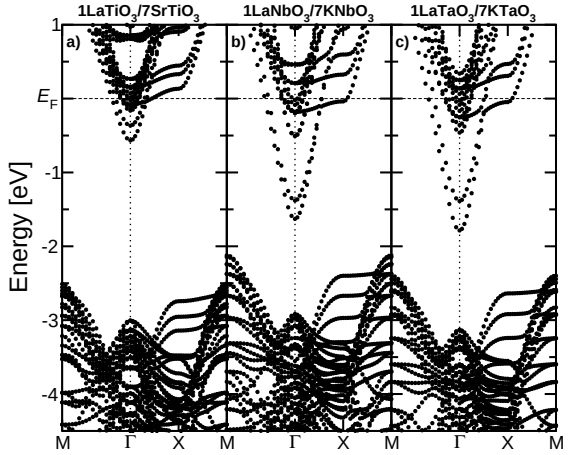

FIG. 2. Electronic band structure for (a) 1 $LaTiO_3$/7 $SrTiO_3$, (b) 1 $LaNbO_3$/7 $KNbO_3$ and (c) 1 $LaTaO_3$/7 $KTaO_3$ emphasizing the partially occupied states near the Fermi surface.

Nb. All superlattice calculations employed an 80 Ry cutoff and an 8×8×1 k-point mesh. Comparisons were made with a prototypical 2DEG system, 1 $LaTiO_3$/7 $SrTiO_3$. In all calculations, the in-plane lattice constants were constrained to the theoretical value of the majority component (i.e. KXO_3 or $SrTiO_3$) and the out-of-plane, c, lattice vector was optimized within the P4mm space group with 1×1 in-plane periodicity. Simultaneously, all ionic coordinates were relaxed until the Hellman-Feynman forces were less than 8 meV/Å. The computed bulk $KNbO_3$, $KTaO_3$, and $SrTiO_3$ cubic lattice constants of 3.951 Å, 3.945 Å, and 3.855 Å, respectively are in typical LDA agreement with the experimental values of 4.000 Å, 3.988 Å and 3.901 Å, respectively. (Note: these values were obtained using standard LDA, i.e. without the inclusion of a Hubbard U). For all heterostructure calculations, a Hubbard U=5 eV for B-cation d-states was found to be appropriate. Similar U values were used in previous studies of $LaTiO_3$/$SrTiO_3$ [15, 22]. For the $LaXO_3$/KXO_3 systems test calculations were also performed for U=3 and 8 eV. All three values of U yielded essentially the same results (see supplementary figures 1 and 2). Band effective masses were computed using quadratic fits of the partially occupied bands.

Figure 1 depicts the density of states (DOS) for bulk $SrTiO_3$, bulk $KTaO_3$, 1 $LaTiO_3$/7 $SrTiO_3$, 1 $LaNbO_3$ /7 $KNbO_3$ and 1 $LaTaO_3$/7 $KTaO_3$ superlattices. Both $SrTiO_3$ and $KTaO_3$, using LDA (i.e. no Hubbard U), have relatively large band gaps of 1.7 and 1.8 eV, respectively. Although smaller than experiment, these are consistent with LDA's underestimation of oxide band gaps. In agreement with previous studies, 1 $LaTiO_3$/7 $SrTiO_3$ has occupied states just below the Fermi level, E_F, that sum to 1 electron (or rather 0.5 e^-/interface unit cell) [15]. The electronic band structure plot (Fig. 2a) indicates that they directly contribute to transport (i.e. cross the Fermi level).

An analysis of the orbital projected DOS indicates that these states are derived mainly from Ti t_{2g} states, with the two lowest energy, light electron, bands coming almost entirely from d_{xy} orbitals on the interfacial Ti ions and the remaining occupied states being a mixture of t_{2g} states on all of the Ti cations. More importantly, in 1 $LaNbO_3$/7 $KNbO_3$ and 1 $LaTaO_3$/7 $KTaO_3$ these occupied electronic states sum up to exactly 2 electrons (i.e. 1 e^- / interface unit cell). An examination of the electronic band structure shows that these bands define the Fermi surface (see Fig. 2b and c). Orbital projected DOS indicate that they are derived mainly from the B-cation d-states (Nb/Ta) with dominant electronic contributions arising from partially occupied d_{xy} orbitals of B-cations at the LaO interface. In all three heterostructures light electronic bands crossing E_F are parabolic around Γ and heavy bands extend along the Γ-X direction. This is a characteristic feature of 2DEGs and is consistent with recent angle-resolved photoemission spectroscopy (ARPES) results for 2DEGs at $SrTiO_3$ and $KTaO_3$ surfaces [9, 17, 30].

Figure 3a displays the spatial distribution of the conduction electrons (i.e. arising from states between E_F and ∼ -1.8 eV) as a function of distance away from the LaO layer. Similar to previous theoretical and experimental results for 2DEGs at heterointerfaces and the $SrTiO_3$ surface we find a build-up of charge of roughly 0.22 electrons on interfacial Ti cations in the 1 $LaTiO_3$/7 $SrTiO_3$ superlattice [14–19]. (Note: the total atom projected DOS adds up to 0.95 e^- and is scaled to unity in the plots.) This charge quickly decays to 0.06 electrons in the center of the slab, indicating a decay length of roughly 3-4 unit cells. On the other hand, we observe that the $LaNbO_3$/$KNbO_3$ and $LaTaO_3$/$KTaO_3$

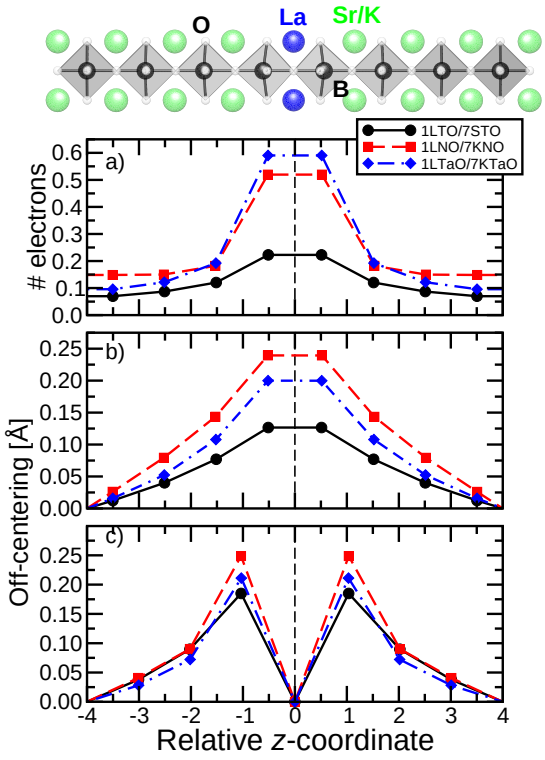

FIG. 3. (color online) [top] Representative 2-dimensional projection of a relaxed superlattices. (a) Charge distribution and (b) magnitude of B- and (c) A-cation off-centering as a function of relative z-coordinate for the superlattices studied. All distances are relative to LaO planes.

heterostructures have a build-up of 0.52 and 0.60 e$^-$s on the interfacial Nb and Ta ions, respectively. (Again the projected DOS only sums to 1.8 e$^-$s and is uniformly scaled to 2.0). Surprisingly, discernible differences in the decay of charge away from the LaO interface are seen. In $LaNbO_3/KNbO_3$, there is still roughly 0.15 e$^-$/unit cell area in the bulk region, whereas the charge density in $LaTaO_3/KTaO_3$ drops off much more sharply, falling to less than 0.1 e$^-$/unit cell area. This deviation may be linked to the dielectric constants. Model Hamiltonian calculations indicate that larger dielectric constants induce a greater spread of electrons away from the interface [35, 36]. $KTaO_3$ and $SrTiO_3$ have very similar dielectric constants [37, 38], while $KNbO_3$ has a much stronger dependence of dielectric constant on phase [39]. In fact, tetragonal $KNbO_3$ has a dielectric constant that is a few orders of magnitude greater than $SrTiO_3$ and $KTaO_3$, making the observed behavior reasonable. Regardless, these results clearly indicate a significant enhancement in the concentration of electrons near the interface for III-III/I-V heterostructure relative to the III-III/II-IV system.

In accordance with the observed interfacial electronic reconstruction we find considerable polar distortions of the A- and B-cations away from the LaO layer. These

TABLE I. Structural parameters and relative effective masses for the heterostructures studied. a_o, c/a and m^*/m_e denote the cubic lattice parameter, c/a ratio and the relative effective masses of the two lowest energy partially occupied bands, respectively. Note: the curvature of the electronic structure around Γ is symmetric. i.e. the effective mass along the Γ-X and Γ-M directions are essentially equal and thus only one value is reported for each band.

System	a_o [Å]	c/a	m^*/m_e	
			1	2
1 $LaTiO_3$/7 $SrTiO_3$	3.885	8.117	0.49	0.59
1 $LaNbO_3$/7 $KNbO_3$	3.951	8.085	0.35	0.41
1 $LaTaO_3$/7 $KTaO_3$	3.945	8.009	0.30	0.35

off-center displacements gradually return to zero in the center of the $SrTiO_3$ or KXO_3 layers. (See Fig. 3 [top] for a representative 2 dimensional projection of the atomic structure of a 1/7 heterostructure). Similar to previous DFT results, the magnitude of $SrTiO_3$ off-centering is 0.18 Å and 0.13 Å for the A- and B-cations near the interface, respectively [15, 22]. Figure 3b and 3c show that the magnitudes of the B- and A-cation off-center displacements in the $LaXO_3/KXO_3$ structures are all appreciably larger than those in $LaTiO_3/SrTiO_3$. These larger polar distortions are consistent with the need for larger interfacial polarizations to adequately screen the interfacial charges. Unexpectedly, the $LaTaO_3/KTaO_3$ superlattice while having the larger interfacial charge exhibits smaller polar distortions than $LaNbO_3/KNbO_3$. There are two contributing factors that lead to this discrepancy. First, the magnitude of charge screening in these two materials arising from the differences in their respective dielectric constants - with the lower dielectric constant material being more strongly screened and thus requiring smaller ionic distortions. Second, $KNbO_3$, unlike $KTaO_3$, has a polar ground state which may be more favorable to inducing polar distortions. This is further supported by the fact that the $LaTaO_3/KTaO_3$ system retains a cubic average lattice parameter (c/a=1.001), while the $LaNbO_3/KNbO_3$ is tetragonally distorted (c/a=1.010; close to the experimental c/a=1.016). The polar nature of the $KNbO_3$ structure may be more advantageous for controlling interface conductivity through electric field switching [21, 40].

Finally, table I lists the relative band effective masses, m^*/m_e, of the two lowest energy partially occupied bands (see Fig. 2). Remarkably, the computed m^* values for $SrTiO_3$, are in excellent agreement with ARPES measurements of $SrTiO_3$ surface 2DEGs (0.5 - 0.6 m_e) [30]. While the origin of $SrTiO_3$ surface 2DEGs is attributed to oxygen vacancies, this result is indicative of characteristic electronic structure features. It should be pointed out that La doped $SrTiO_3$ has a considerably higher effective mass ($m^*/m_e > 1$) and that the band effec-

tive masses predicted here neglects some correlation effects. Moreover, the 1 LaXO$_3$/7 KXO$_3$ structures were found to have significant decreases in m^* for these bands (which dominate the electron density at the interfaces), implying possible increases in carrier mobilities in the III-III/I-V superlattices. Once again, these values correlate well with recent ARPES experiments for $KTaO_3$ surface 2DEGs which measure a band effective mass of 0.30 m_e [9]. This is exceptional agreement, especially when considering the fact that the $KTaO_3$ surface 2DEG has half the number of electrons as the heterostructures discussed here and is indicative of the point that the band effective mass of the oxide 2DEG is an intrinsic property of the bulk component material. Of course, this larger concentration of electrons may lead to decreased mobilities either due to shorter scattering lifetimes, τ, or increased electron-electron correlations. However, recently we demonstrated that the carrier mobilities at a δ-doped interface may be enhanced through fractional doping (i.e. less than one full doping layer at the interface) [41]. The optimal dopant level was found to be 50% for $LaTiO_3/SrTiO_3$ heterostructure. This translates into a 50 % decrease in the carrier concentration. As such, optimal fractional δ-doping of the above structures would allow for much higher carrier concentrations with higher mobilities (coupled to the higher band effective masses). Hence, improvements in electron mobilities, μ_e, would be strongly linked to changes in m^* (where $\mu_e = e\tau/m^*$).

In summary, using first principles methods, it is demonstrated that superlattices comprising I-V ($K^{1+}[Nb/Ta]^{5+}O_3$) and III-III ($La^{3+}[Nb/Ta]^{3+}O_3$) perovskites have twice the interfacial charge densities of III-III/II-IV($SrTiO_3/LaTiO_3$) superlattices. Here, the flexibility of multivalent cations, like Nb and Ta, leads to an intrinsic limit of 1 e^- per interface unit cell, twice that of previously studied III-III/II-IV and I-V/III-III [21, 42] superlattices. Also, changes in electron band effective masses (with no change in dopant levels) imply that further enhancements in mobilities may be achievable. Correlations between the band effective masses of surface 2DEGs and these heterostructures highlight the characteristic behavior of 2DEGs derived from d^0 transition metal oxides and a combined approach may be fundamental to understanding the underlying physics of electron confinement [9, 17, 30]. In addition, deviations in polar distortions indicate that polar, high dielectric constant materials like $KNbO_3$ may be more suitable for applications based on electric field switching of interfacial charge carrier concentrations [21, 40]. Naturally, synthetic limitations related to effectively reducing ions like Ta^{5+} to Ta^{3+} may exist. A feasible route may be to substitute interfacial Ta cations with a cation, like V, that is more easily reduced. Ultimately, these results present a chemically intuitive framework (in the absence of factors such as O vacancies) through which intrinsic carrier concentrations, and perhaps even carrier mobilities, of oxide heterostructure 2DEGs can be tuned and may be useful in device engineering [6] and in understanding and controlling quantum phenomena due to electron confinement.

V.R.C. would like to acknowledge helpful discussions with C. Bridges, C. Cantoni, H. N. Lee, S. Okamoto, D. Parker, W. Siemons and D. Xiao. This work was supported by the Materials Sciences and Engineering Division, Office of Basic Energy Sciences, U.S. Department of Energy. This research used resources of the National Energy Research Scientific Computing Center, supported by the Office of Science, U.S. Department of Energy under Contract No. DEAC02-05CH11231.

* coopervr@ornl.gov

[1] A. Ohtomo, D. A. Muller, J. L. Grazul, and H. Y. Hwang, Nature **419**, 378 (2002).
[2] S. Thiel, G. Hammerl, A. Schmehl, C. W. Schneider, and J. Mannhart, Science **313**, 1942 (2006).
[3] A. Brinkman, M. Huijben, M. van Zalk, J. Huijben, U. Zeitler, J. C. Maan, W. G. van der Wiel, G. Rijnders, D. H. A. Blank, and H. Hilgenkamp, Nat. Mater. **6**, 493 (2007).
[4] K. v. Klitzing, G. Dorda, and M. Pepper, Phys. Rev. Lett. **45**, 494 (1980).
[5] T. Ando, A. B. Fowler, and F. Stern, Rev. Mod. Phys. **54**, 437 (1982).
[6] J. Mannhart and D. G. Schlom, Science **327**, 1607 (2010).
[7] H. Ohta, S. Kim, Y. Mune, T. Mizoguchi, K. Nomura, S. Ohta, T. Nomura, Y. Nakanishi, Y. Ikuhara, M. Hirano, H. Hosono, and K. Koumoto, Nat. Mater **6**, 129 (2007).
[8] S. LaShell, B. A. McDougall, and E. Jensen, Phys. Rev. Lett. **77**, 3419 (1996).
[9] P. D. C. King, R. H. He, T. Eknapakul, P. Buaphet, S.-K. Mo, Y. Kaneko, S. Harashima, Y. Hikita, M. S. Bahramy, C. Bell, Z. Hussain, Y. Tokura, Z.-X. Shen, H. Y. Hwang, F. Baumberger, and W. Meevasana, Phys. Rev. Lett. **108**, 117602 (2012).
[10] G. A. Baraff, J. A. Appelbaum, and D. R. Hamann, Phys. Rev. Lett. **38**, 237 (1977).
[11] W. A. Harrison, E. A. Kraut, J. R. Waldrop, and R. W. Grant, Phys. Rev. B **18**, 4402 (1978).
[12] H. Chen, A. M. Kolpak, and S. Ismail-Beigi, Adv. Mater. **22**, 2881 (2010).
[13] H. W. Jang, D. A. Felker, C. W. Bark, Y. Wang, M. K. Niranjan, C. T. Nelson, Y. Zhang, D. Su, C. M. Folkman, S. H. Baek, S. Lee, K. Janicka, Y. Zhu, X. Q. Pan, D. D. Fong, E. Y. Tsymbal, M. S. Rzchowski, and C. B. Eom, Science **331**, 886 (2011).
[14] W. Siemons, G. Koster, H. Yamamoto, W. A. Harrison, G. Lucovsky, T. H. Geballe, D. H. A. Blank, and M. R. Beasley, Phys. Rev. Lett. **98**, 196802 (2007).
[15] S. Okamoto, A. J. Millis, and N. A. Spaldin, Phys. Rev. Lett. **97**, 056802 (2006).
[16] S. Okamoto and A. J. Millis, Nature **428**, 630 (2004).
[17] A. F. Santander-Syro, O. Copie, T. Kondo, F. Fortuna, S. Pailhes, R. Weht, X. G. Qiu, F. Bertran, A. Nicolaou, A. Taleb-Ibrahimi, P. Le Fevre, G. Herranz, M. Bibes,

N. Reyren, Y. Apertet, P. Lecoeur, A. Barthelemy, and M. J. Rozenberg, Nature **469**, 189 (2011).
[18] C. Cantoni, J. Gazquez, F. M. Granozio, M. P. Oxley, M. Varela, A. R. Lupini, S. J. Pennycook, C. Aruta, U. S. di Uccio, P. Perna, and D. Maccariello, (unpublished).
[19] M. Takizawa, S. Tsuda, T. Susaki, H. Y. Hwang, and A. Fujimori, arXiv:1106.3619v1.
[20] J. S. Kim, S. S. A. Seo, M. F. Chisholm, R. K. Kremer, H.-U. Habermeier, B. Keimer, and H. N. Lee, Phys. Rev. B **82**, 201407(R) (2010).
[21] Y. Wang, M. K. Niranjan, S. S. Jaswal, and E. Y. Tsymbal, Phys. Rev. B **80**, 165130 (2009).
[22] D. R. Hamann, D. A. Muller, and H. Y. Hwang, Phys. Rev. B **73**, 195403 (2006).
[23] A. Ohtomo and H. Y. Hwang, Nature **427**, 423 (2004).
[24] N. Nakagawa, H. Y. Hwang, and D. A. Muller, Nat. Mater. **5**, 204 (2006).
[25] R. Pentcheva and W. E. Pickett, Phys. Rev. Lett. **102**, 107602 (2009).
[26] N. C. Bristowe, E. Artacho, and P. B. Littlewood, Phys. Rev. B **80**, 045425 (2009).
[27] M. Stengel and D. Vanderbilt, Phys. Rev. B **80**, 241103 (2009).
[28] P. Perna, D. Maccariello, M. Radovic, U. S. di Uccio, I. Pallecchi, M. Codda, D. Marr, C. Cantoni, J. Gazquez, M. Varela, S. J. Pennycook, and F. M. Granozio, Appl. Phys. Lett. **97**, 152111 (2010).
[29] A. Kalabukhov, R. Gunnarsson, J. Börjesson, E. Olsson, T. Claeson, and D. Winkler, Phys. Rev. B **75**, 121404 (2007).
[30] W. Meevasana, P. D. C. King, R. H. He, S. K. Mo, M. Hashimoto, A. Tamai, P. Songsiriritthigul, F. Baumberger, and Z. X. Shen, Nat. Mater. **10**, 114 (2011).
[31] V. I. Anisimov, J. Zaanen, and O. K. Andersen, Phys. Rev. B **44**, 943 (1991).
[32] D. Vanderbilt, Phys. Rev. B **41**, 7892(R) (1990).
[33] M. Cococcioni and S. de Gironcoli, Phys. Rev. B **71**, 035105 (2005).
[34] P. Giannozzi, *et al.*, J. Phys.: Cond. Matt. **21**, 395502 (2009).
[35] S. Okamoto and A. J. Millis, Phys. Rev. B **70**, 075101 (2004).
[36] S. S. Kancharla and E. Dagotto, Phys. Rev. B **74**, 195427 (2006).
[37] M. D. Agrawal and K. V. Rao, J. Phys. C: Solid State Phys. **3**, 1120 (1970).
[38] G. Rupprecht and R. O. Bell, Phys. Rev. **135**, A748 (1964).
[39] G. Shirane, H. Danner, A. Pavlovic, and R. Pepinsky, Phys. Rev. **93**, 672 (1954).
[40] A. D. Caviglia, S. Gariglio, N. Reyren, D. Jaccard, T. Schneider, M. Gabay, S. Thiel, G. Hammerl, J. Mannhart, and J. M. Triscone, Nature **456**, 624 (2008).
[41] W. S. Choi, S. Lee, V. R. Cooper, and H. N. Lee, (2012), (unpublished).
[42] E. D. Murray and D. Vanderbilt, Phys. Rev. B **79**, 100102 (2009).